



Studies of 2-azaazulenium derivatives – 3: The nature of electron transitions and spectral properties of styryl dyes containing terminal groups of different types

Julia L. Bricks^a, Alona V. Stanova^{b,*}, Aleksey B. Ryabitsky^c, Valeriy M. Yashchuk^b, Aleksey D. Kachkovsky^a

^a Department of Colour and Structure of Organic Compounds, Institute of Organic Chemistry, National Academy of Sciences of Ukraine, 5 Murmanska str., 02660 Kyiv, Ukraine

^b Physics Department, Taras Shevchenko National University of Kiev, 4 Glushkova Prosp., 03187 Kyiv, Ukraine

^c Spoluka Chemical Company, 5 Murmanska str., 02660 Kyiv, Ukraine¹

H I G H L I G H T S

- Cyanine dyes explored by spectroscopic methods and quantum chemical calculations.
- Classification of cyanine dyes is proposed basing on the research.
- Features in the absorption spectra of AA dyes caused by the local molecular orbital.

A R T I C L E I N F O

Article history:

Received 20 June 2012

Received in revised form 19 August 2012

Accepted 20 August 2012

Available online 30 August 2012

Keywords:

Absorption

Azaazulenes

Dyes/pigments

Quantum-chemical calculations

NMR spectroscopy

A B S T R A C T

This paper presents the results of a quantum-chemical study of the molecular geometry and electron structure as well as spectral measurements of absorption and ¹³C NMR spectra of dimethylaminostyryls, methoxystyryls, and methylstyryls bearing 2-azaazulenium (AA) moiety in comparison with analogous dyes containing 2-benzimidazolim and 4-pyrylium residues. Based on the analysis of both calculations and experimental data, it was concluded that these types of extremely unsymmetrical cyanines differ between each other only slightly in the ground state with respect to the charge distribution and molecular geometry while their spectral properties reveal a considerable difference between dimethylaminostyryls and methoxystyryls due to the lowest disposition of the lone electron pair level of the oxygen atom and hence, limiting basicity of the p-methoxyphenylene residue. It was shown that appearance of a high-positioned local level generated by AA terminal group caused the inversion of the delocalized and quasi-local electron transitions in AA-methoxystyryl and hence drastic changes in its absorption spectrum.

© 2012 Elsevier B.V. All rights reserved.

1. Introduction

Styryl dyes have numerous successful applications [1]. For example, they can be used as fluorescence probes, laser active and passive components, as optical sensitizers, as recording media (optical disks) and potential objects for molecular electronics.

One of the most significant problems of the color theory of polymethine dyes is investigation of the dependency of the electronic transitions and π -electron density distribution upon the electron asymmetry degree of dye molecules [2–9]. It was found both experimentally [2,5,6,10] and theoretically [3,4,11–14] that going from symmetrical cyanine dyes to chemically unsymmetrical cyanines affects considerably their spectral properties. We have reported a study of properties of symmetrical and unsymmetrical

monomethine and trimethine cyanine derivatives of 2-azaazulene in our preceding papers [15,16]. There we have shown that 2-azaazulenium (AA) residue can be treated as a low basic terminal group. Its donor properties are provided by the participation not of the highest occupied molecular orbital (HOMO) but of the next HOMO-1, in contrast to the typical Brooker's terminal residues with their donor HOMOs. It enables us to propose a new classification of terminal groups of cyanine dyes and hence a classification of symmetrical and unsymmetrical cyanines. It was shown that the nature of the highest electron transitions (delocalized or local) in cyanine dyes depends on the relative dispositions of local and delocalized molecular orbitals (MOs). In unsymmetrical trimethine cyanines containing terminal groups of different types, unusual spectral properties could occur, for example, the negative deviation.

In our previous paper devoted to the properties of styryls and their heteroanalogues [17], we have shown that p-methoxyphenylene residue in methoxystyryls should be considered as a special type of the terminal group with an extremely low electron donor

* Corresponding author. Tel.: +380 671949208.

E-mail addresses: jbricks@ioch.kiev.ua (J.L. Bricks), diakova_a@ukr.net (A.V. Stanova).

¹ www.lifechemicals.com.

level, which remains under the highest occupied level of the chain. It leads to a considerable hypsochromic shift of the first absorption maxima of methoxystyryls relatively to styryls. The quantum-chemical calculations have shown that the nature of the second transition $S_0 \rightarrow S_2$ in methoxystyryls have been changed, in comparison with corresponding dimethylamino styryls.

At the same time, earlier it was reported that in symmetrical and unsymmetrical polymethine dyes with AA terminal groups specific electron transitions from local MOs take place [15,16]. The direct experimental observation of the local transitions in absorption spectra was not often possible because they could be hidden under the high-intensive band connected with the first delocalized transition. For example, it is in contrast to the spectra of pyrylocyanines and their heteroanalogues, when the local transitions are revealed themselves as separate low-intensive spectral bands. It could be expected that the combination of AA terminal group, with its local electron level, and a specific p-methoxyphenyl group in methoxystyryl will result in appearance of local transitions.

This paper presents the results of a quantum-chemical study of the electron structure and electron transitions features as well as spectral measurements of absorption and NMR spectra of dimethylaminostyryls (DMA-styryls), methoxystyryls (OMe-styryls), and methylstyryls (Me-styryls) bearing 2-azaazulenium moiety in comparison with analogous dyes containing 2-benzimidazolium and 4-pyrylium residues.

2. Experimental section

2.1. Measurements and quantum-chemical calculations

UV/Vis absorption spectra were recorded on Shimadzu UV-3100 spectrophotometer.

All NMR measurements were carried out on Varian GEMINI 2000 spectrometer with ^1H and ^{13}C frequencies of 400.07 and 100.61 MHz, respectively at 293 K. Tetramethylsilane was used as a standard for δ scale calibrating. ^1H NMR spectra were recorded with spectral width 8000 Hz and numbers of points 32000; ^{13}C NMR spectra were recorded with spectral width 30,000 Hz and numbers of points 128,000. ^1H – ^1H COSY [18] spectra were acquired into 2048 (F2) and 512 (F1) time-domain data matrix and 2048 (F2) \times 2048 (F1) frequency-domain matrix after zero-filling. NOESY [19] spectra were acquired, if necessary, with parameters similar to COSY spectra. Mixing times were determined preliminarily from T_1 -measurement experiment for each sample by conventional inversion-recovery method. Heteronuclear chemical shift correlation (HETCOR) [20] was used to determine ^1H – ^{13}C attachment with 2048 (F2) \times 256 (F1) time-domain matrix and 2048 (F2) \times 1024 (F1) frequency-domain matrix after zero-filling. The average value of one bond constant J_{CH} was set to 140 Hz. HETCOR for determination long range correlation had very similar parameters and average value of multibond C–H coupling constant was set to 8 Hz.

The quantum-chemical calculations were carried out to study the dependence of the electron structure and electron transitions on molecular constitution. The equilibrium geometry of dye molecules in the ground state was optimized using GAUSSIAN03 [21] program set with DFT approximation. A functional B3LYP [22] was chosen, in combination with the standard 6-31G(d,p) basis set. In case of need for some structures the conformational analysis was carried out using scanning of the potential energy surface to search the optimal conformation with the energy minimum. Charge distribution in atoms was calculated using the theory of Natural Bond Orbital analysis (NBO) [23]. The electron transition characteristics were calculated using two methods: TD DFT/6-

31G(d,p)/B3LYP method with (TD DFT in text) and semi-empirical AM1 method.

2.2. Synthesis

A series of styryl dyes reported here was synthesized by conventional cyanine chemistry approach [6,24]. This approach involves heating a mixture of *p*-R-substituted benzaldehydes and the corresponding quaternary salts of nitrogen containing heterocycles or 4-methyl-2,6-di(*tert*-Bu/or Ph)-pyrylium salts in an appropriate solvent. Structures of all synthesized dyes see in Table 1.

The purity of the dyes have been checked by TLC and their structures were confirmed by NMR (^1H NMR and ^{13}C NMR) and elemental analysis.

Starting materials and solvents for the synthesis and spectroscopic measurements were purchased from Sigma–Aldrich.

AA-Styryls (General procedure for AA dyes): A solution of 1 mmol of 2-butyl-1,3,6-trimethyl-cyclohepta[c]pyrrolium tetrafluoroborate and 1.5 mmol of *p*-dimethylamino benzaldehyde, or *p*-anisaldehyde, or *p*-methylbenzaldehyde in dimethylsulfoxide (2 mL) was heated at 50 °C for 15–20 min. The solvent was evaporated in vacuum. The residue was triturated with diethyl ether (5 \times 5 mL) and dissolved in ethanol (2 mL). After cooling to room temperature the precipitated dye was filtered off, washed with diethyl ether (2 \times 10 mL) and purified by recrystallization from ethanol.

2-Butyl-6-[2-[4-(dimethylamino)phenyl]vinyl]-1,3-dimethyl cyclohepta[c]pyrrolium tetrafluoroborate AA-DMA was obtained from 2-butyl-1,3-trimethylcyclohepta[c] pyrrolium tetrafluoroborate and *p*-dimethylaminobenzaldehyde [25].

2-Butyl-6-[2-(4-methoxyphenyl)vinyl]-1,3-dimethylcyclohepta [c] pyrrolium tetrafluoroborate AA-OMe was obtained from 2-butyl-1,3-trimethylcyclohepta[c] pyrrolium tetrafluoroborate and *p*-anisaldehyde [25].

2-Butyl-6-[2-(4-methylphenyl)vinyl]-1,3-dimethylcyclohepta [c]pyrrolium tetrafluoroborate AA-Me was obtained from 2-butyl-1,3-trimethylcyclohepta[c] pyrrolium tetrafluoroborate and *p*-methylbenzaldehyde was obtained from 2-butyl-1,3-trimethylcyclohepta[c] pyrrolium tetrafluoroborate and *p*-methylbenzaldehyde. Yield 34%, m.p. 159–162 °C (decomposition); λ_{max} = 464 nm, ϵ = 17100 M $^{-1}$ cm $^{-1}$ (in acetonitrile). ^1H NMR (CDCl $_3$, 400 MHz) δ : 8.55 (d, J = 10.3 Hz, 2H, AAz), 7.65 (d, J = 16.5 Hz, 1H, –CH=CH–), 7.59 (d, J = 10.3 Hz, 2H, AAz), 7.51 (d, J = 8.0 Hz, 1H, C $_6$ H $_4$), 7.22 (d, J = 8.0 Hz, C $_6$ H $_4$), 7.07 (d, J = 16.5 Hz, –CH=CH–), 4.25–4.18 (m, 2H, NCH $_2$), 2.75 (s, 6H, 2 \times CH $_3$ AAz), 2.40 (s, 3H, C $_6$ H $_4$ CH $_3$), 1.73–1.63 (m, 2H, NCH $_2$ CH $_2$), 1.49–1.36 (m, 2H, CH $_3$ CH $_2$), 0.89 (t, J = 7.3 Hz, 3H, CH $_3$ CH $_2$). Elemental analysis calcd. (%) for C $_{24}$ H $_{28}$ BF $_4$ N (417.29): C 69.08, H 6.76, N 3.36%; found: C 69.32, H 6.44, N 3.58%.

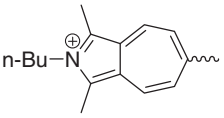
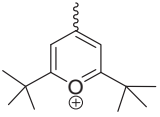
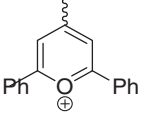
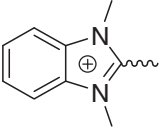
Preparation of Py-*t*Bu-styryl dyes. A solution of 2,6-di-*tert*-butyl-4-methylpyrylium perchlorate (1 mmol) and *p*-dimethylaminobenzaldehyde, or *p*-anisaldehyde, or *p*-methylbenzaldehyde (1.1 mmol) in acetonitrile (2 mL) was heated for 1 h at 130 °C. After cooling, the reaction mixture was triturated with diethyl ether (50 mL) and the obtained solid was filtered and crystallized from the mixture of ethanol–diethyl ether (1:2).

2,6-di-*tert*-Butyl-4-[2-[4-(dimethylamino)phenyl]vinyl]pyrylium perchlorate, Py-*t*Bu-DMA was described in [25].

2,6-di-*tert*-Butyl-4-[2-(4-methoxyphenyl)vinyl]pyrylium perchlorate Py-*t*Bu-OMe was described in [25].

2,6-di-*tert*-Butyl-4-[2-(4-methylphenyl)vinyl]pyrylium perchlorate Py-*t*Bu-Me. Yield 45%, m.p. 198–200 °C (decomposition); λ_{max} = 411 nm, ϵ = 32300 M $^{-1}$ cm $^{-1}$ (in acetonitrile). ^1H NMR (CDCl $_3$, 400 MHz) δ : ^1H NMR (CDCl $_3$, 400 MHz) δ : 8.31 (d,

Table 1
Spectral properties of styryl dyes.

Het ⁺ (X [−])	R	Dye abbreviation	Absorption spectra, λ_{max} (nm) ($\epsilon \times 10^{-4}$, (M ^{−1} cm ^{−1})) in CH ₃ CN
 (BF ₄)	N(CH ₃) ₂ OCH ₃ CH ₃	AA-DMA	681 (4.82), 334 (1.56)
		AA-OMe	656 (0.27), 497 (2.39), 304 (1.68)
		AA-Me	660 (0.26), 464 (1.71), 338 (1.19), 295 (1.71)
 (BF ₄)	N(CH ₃) ₂ OCH ₃ CH ₃	Py-tBu-DMA	577 (7.87), 299 (1.26)
		Py-tBu-OMe	446 (3.78), 307 (0.90)
		Py-tBu-Me	411 (3.23), 309 (1.11)
 (I)	N(CH ₃) ₂ OCH ₃	Py-Ph-DMA	628 (9.46), 386 (2.18)
		Py-Ph-OMe	481 (5.9), 415 (3.08), 271 (2.93)
 (I)	N(CH ₃) ₂ OCH ₃ CH ₃	Blm-DMA	397 (1.69), 281 (1.45)
		Blm-OMe	343 (2.74)
		Blm-Me	329 (3.23)

$J = 14.8$ Hz, 1H, $-\text{CH}=\text{CH}-$), 7.90 (s, 2H, Py), 7.78 (d, $J = 8.0$ Hz, 2H, C₆H₄), 7.44 (d, $J = 14.8$ Hz, 2H, $-\text{CH}=\text{CH}-$), 7.20 (d, $J = 8.0$ Hz, 2H, C₆H₄), 2.37 (s, 3H, CH₃C₆H₄), 1.49 (s, 18H, $2 \times t\text{-Bu}$). Elemental analysis calcd. (%) for C₂₂H₂₉BF₄O (396.27): C 66.68, H 7.38%; found: C 66.42, H 7.30%.

4-{2-[4-(dimethylamino)phenyl]vinyl}-2,6-diphenylpyrylium perchlorate Py-Ph-DMA was described in [26].

4-[2-(4-methoxyphenyl)vinyl]-2,6-diphenylpyrylium perchlorate Py-Ph-OMe was described in [27].

2-{2-[4-(dimethylamino)phenyl]vinyl}-1,3-dimethyl-1H-3,1-benzimidazol-3-ium iodide Blm-DMA. A mixture of 1,2,3-trimethyl-1H-3,1-benzimidazol-3-ium iodide (0.58 g, 2 mmol), p-dimethylaminobenzaldehyde (0.4 g, 2.68 mmol), and DBU (five drops) was heated in pyridine (7 mL) at 110 °C for 3 h. After cooling the orange precipitate was filtered off, washed with pyridine (2 mL), hot water (10 mL), methanol (5 mL), diethyl ether (5 mL), dried and purified by recrystallization from DMSO. Yield 0.52 g (62%); m.p. 297–300 °C (decomposition); ¹H NMR (400 MHz, [D₆]DMSO, 25 °C, TMS): $\delta = 8.00\text{--}7.94$ (m, 2H, Blm), 7.78 (d, $J = 8.9$ Hz, 2H, C₆H₄), 7.74 (d, $J = 16.5$ Hz, 1H, $-\text{CH}=\text{CH}-$), 7.66–7.60 (m, 2H, Blm), 7.19 (d, $J = 16.5$ Hz, 1H, $-\text{CH}=\text{CH}-$), 6.78 (d, $J = 8.9$ Hz, 2H, C₆H₄), 4.11 (s, 6H, $2 \times \text{CH}_3$ Blm), 3.05 (s, 6H, N(CH₃)₂). Elemental analysis calcd. (%) for C₁₉H₂₂N₃ (419.3): I 30.27, N 10.02; found: I 30.05, N 10.24.

2-[2-(4-methoxyphenyl)vinyl]-1,3-dimethyl-1H-3,1-benzimidazol-3-ium iodide Blm-OMe. A mixture of 1,2,3-trimethyl-1H-3,1-benzimidazol-3-ium iodide (0.58 g, 2 mmol), p-anisaldehyde (0.544 g, 4 mmol) and piperidine (0.1 g) was heated in pyridine (7 mL) at 130 °C for 8 h. Then p-anisaldehyde (0.27 g, 2 mmol) was added, and the heating was continued for 6 h. After cooling the precipitate was filtered off, washed with hot water (10 mL), ethanol (5 mL), diethyl ether (2×5 mL), dried and purified by recrystallization from DMSO (twice). Yield 0.450 g (55%); m.p. 272–275 °C (decomposition); ¹H NMR (400 MHz, [D₆]DMSO, 25 °C, TMS): $\delta = 8.07\text{--}8.01$ (m, 2H, Blm), 7.93 (d, $J = 8.8$ Hz, 2H, C₆H₄), 7.81 (d, $J = 16.7$ Hz, 1H,

$-\text{CH}=\text{CH}-$), 7.70–7.65 (m, 2H, Blm), 7.41 (d, $J = 16.7$ Hz, 1H, $-\text{CH}=\text{CH}-$), 7.11 (d, $J = 8.8$ Hz, 2H, C₆H₄), 4.14 (s, 6H, $2 \times \text{CH}_3$ Blm), 3.85 (s, 3H, OCH₃). Elemental analysis calcd. (%) for C₁₇H₁₆N₂O: I 32.44, N 7.16; found: I 32.27, N 7.12.

2-[2-(4-methylphenyl)vinyl]-1,3-dimethyl-1H-3,1-benzimidazol-3-ium iodide Blm-Me was obtained in a similar way from 1,2,3-trimethyl-1H-3,1-benzimidazol-3-ium iodide (0.58 g, 2 mmol) and p-methylbenzaldehyde (0.6 g, 5 mmol). Purification was by recrystallization from DMSO (twice). Yield 0.370 g (47%); m.p. 298–299.5 °C (decomposition); ¹H NMR (400 MHz, [D₆]DMSO, 25 °C, TMS): $\delta = 8.03\text{--}7.98$ (m, 2H, Blm), 7.74–7.67 (m, 3H, Blm $-\text{CH}=\text{CH}-$), 7.17 (d, $J = 8.2$ Hz, 2H, C₆H₄), 6.77 (d, $J = 12.7$ Hz, 1H, $-\text{CH}=\text{CH}-$), 3.73 (s, 6H, $2 \times \text{CH}_3$ Blm), 2.29 (s, 3H, CH₃). Elemental analysis calcd. (%) for C₁₈H₁₉N₂: I 32.52, N 7.18; found: I 32.32, N 7.25.

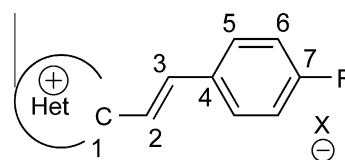
3. Results and discussion

3.1. Objects and their spectral properties

The spectral properties of studied dyes are presented in Table 1. Scheme 1 below demonstrates a general structure of investigated dyes.

3.2. Optimized molecular geometry in the ground state

The quantum-chemical calculations have shown that almost all molecules are practically planar, which is typical for conjugated

**Scheme 1.**

systems. Only both phenyl substituents in the Py-Ph-dyes lie out of the main plane of the pyrylium heterocycle through approximately 25° (*ab initio* or Hartree–Fock method (HF)), whereas the DFT method gives essentially minor value of the torsion angle 10.5° . Blm residues in the corresponding dyes also turned out the main chromophore because of considerable sterical hindrances: through 40° in the case of Blm-DMA dye and through 44° in the case of dye Blm-OMe.

In contrast to symmetrical AA-cyanines with their practically equalized lengths of carbon–carbon bonds in the open chain [4,5,11] a regular alternation of lengths of the neighboring bonds in the chromophore of unsymmetrical AA-DMA and AA-OMe is observed. As an illustration, the bond lengths values in AA dye molecules are presented in Fig. 1. Bond lengths numeration see in Scheme 2. One can see that not only the bond lengths in the open chain alternated, but the bond lengths in the benzene ring of both dyes also demonstrate the appreciable alternation.

To analyze the dependence of the bond length alternation (BLA) on the topology of the terminal groups, we will use an amplitude Δl_v calculated by the following equation [28]:

$$\Delta l_v = (l_v - l_{v+1}) \quad (1)$$

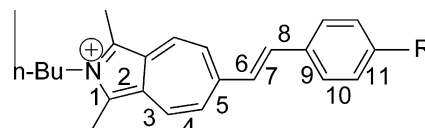
where l_v is the length of the v th bond.

The plot of values $|\Delta l_v|$ versus the numbers of the bond pair along the chromophore for synthesized dye series are pictured in Fig. 2. First of all, one can see that the amplitude of the BLA (Δl_v) in the open chain of methoxystyryls-OMe exceeds this parameter in the branched part (benzene ring); whereas the values Δl_v for the benzene ring and the open chain of styryls-DMA are comparable, especially in the dyes with the low basic variable terminal group R. It has to be noted that the method DFT taking into consideration the electron correlation gives the longer double (formally) bond and hence the less degree of the BLA (Fig. 2).

The analysis of the results of quantum-chemical calculations of all dyes has shown that parameter Δl_v for the bond lengths in the open chain is more sensitive (in comparison with the bonds in the benzene ring) to the donor strength of the variable residue R. For example, the DFT method gives the following order of value Δl_v for the bond pair 2 (Fig. 2a, $\gamma = 2$) in the open chain of the DMA-styryls:

$$\text{Blm} > \text{AA} > \text{Py-t-Bu} \approx \text{Py-Ph}$$

It agrees with the conclusion about the low basicity of the AA terminal group drawn in our previous papers [15,16]. It has to be noted that similar regularities for OMe-styryls and Me-styryls are not clearly pronounced. The data obtained by *ab initio* (HF) method have also proved the fact of lower basicity of the AA, in comparison with the high basicity of the Blm residue.



Scheme 2.

3.3. Charge distribution and ^{13}C NMR shifts

In our previous papers we have established that it is observed a considerable cyanine-like alternation of the charges at the neighboring carbon atoms along the chromophore for symmetrical and unsymmetrical derivatives of AA cyanines, what was confirmed experimentally by means of NMR spectroscopy. So, ^{13}C chemical shifts (δ_μ) for the neighboring carbon atoms are dislocated in the opposite fields, what agrees with the calculated electron density values (q_μ) at the atoms.

The same alternations of both atomic charges (q_μ) and the corresponding NMR ^{13}C signals (δ_μ) are obtained for styryl dyes AA-, Py-tBu-, Blm-. The measured chemical shifts of investigated dyes are collected in Table 2, while the alternation of the values Δq_μ and $\Delta \delta_\mu$ calculated by formulae (2) [29], and (3) for the open chain and benzene ring (as a branched chromophore) are pictured in Figs. 3 and 4.

$$\Delta q_\mu = (-1)^\mu (q_\mu - q_{\mu+1}) \quad (2)$$

$$\Delta \delta_\mu = (-1)^\mu (\delta_\mu - \delta_{\mu+1}) \quad (3)$$

A noticeable diminishing of ^{13}C shifts alternation for atoms C1 and C2 in AA-dyes is observed due to a considerable remoteness of these atoms from the heteroatom of the AA heterocycle, unlike this one in the case of Py-tBu- and Blm-dyes.

The calculations gave practically the same magnitudes of parameter Δq_μ , for the pairs of carbon atoms in the benzene ring for the series of the studied dyes. Only the degree of the electron densities alternation for the first pair (DFT, point 1 in Fig. 3a and c) of the atoms (starting from the nearest one to the heteroatom) is higher for the OMe-styryls than for the DMA-styryls.

The maximum differences in the alternation degree Δq_μ for the same pair of atoms in both series of the dyes (DMA- and OMe-styryls) are obtained for the open chain, especially nearly to the variable terminal residues Het (C1). One can see from Fig. 3 that the increasing of the donor properties (or basicity) of the terminal group in the series Py-t-Bu < AA < Blm (independently on the nature of the second end group: $\text{N}(\text{CH}_3)_2$ in DMA-styryls or OCH_3 in OMe-styryl), is accompanied by a regular decreasing of values Δq_μ , as it is evident from the comparison of the first and second

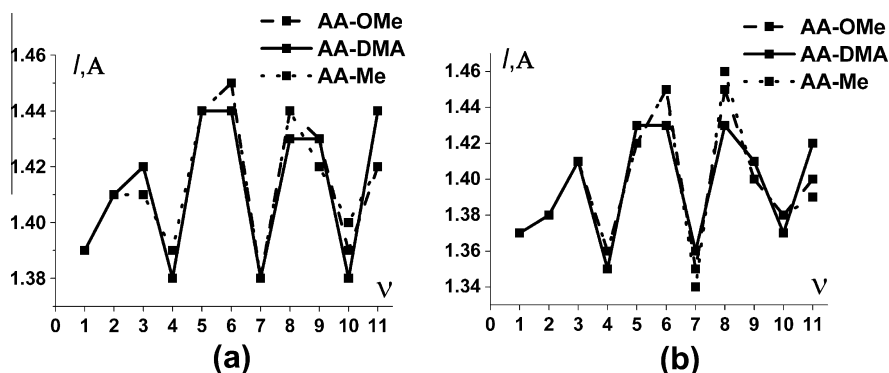


Fig. 1. Bond length values for the dye AA-molecules, calculated using (a) Density-Functional Theory (DFT) method and (b) Hartree-Fock (HF) method; v is the number of the bond.

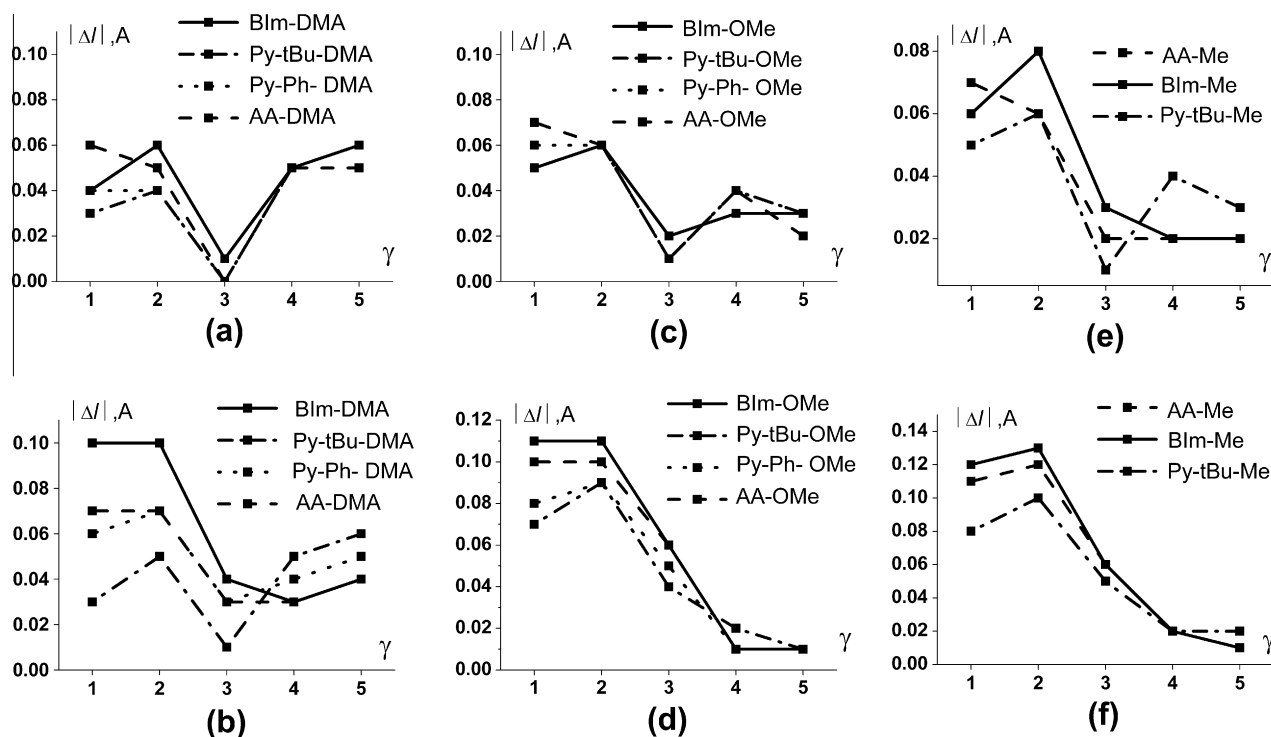


Fig. 2. Alternation of the calculated bond length for studied dyes, (a–e) – DFT method; (b–f) – HF method; γ is the number of the bond pair (Scheme 1 above shows carbon atom numeration for the part of the molecule that used here for calculations).

Table 2
Experimental chemical shifts ^{13}C δ_μ of investigated styryl dyes recorded in $[\text{D}_6]\text{DMSO}$.

Carbon atom number ^a	AA-DMA	AA-OMe	AA-Me	Py-tBu-DMA	Py-tBu-OMe	Py-tBu-Me	BIm-DMA	BIm-OMe	BIm-Me
1	162.76	162.80	162.01	160.75	164.48	165.16	152.17	148.49	148.61
2	129.19	125.72	129.45	116.24	120.35	122.01	100.49	105.02	108.16
3	143.38	146.57	142.86	152.90	151.95	151.73	147.12	146.17	145.88
4	128.30	123.56	132.06	123.14	127.18	131.62	121.61	126.96	131.29
5	131.05	132.59	128.57	134.71	133.09	130.52	130.49	130.46	128.21
6	114.76	112.40	129.48	112.32	114.62	129.81	111.52	114.46	129.78
7	161.97	153.26	141.73	154.48	163.66	143.94	149.00	161.64	140.22

^a The numbering of carbon atoms see Scheme 1.

points in Fig. 3. On the contrary, the alternation of the bond lengths Δl_v increases for the same points in the dye series considered above (Fig. 2).

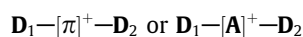
It is reasonable that a similar trend should be observed for the alternation of the chemical shifts, $\Delta\delta_\mu$. Indeed, the alternation of the chemical shifts is seen from Fig. 4 to be appreciable for the two first pairs of atoms in the chromophore, while differences in the magnitudes $\Delta\delta_\mu$ for the rest atom pairs of the conjugated π -system are less (compare Figs. 3 and 4).

Thus, the increasing of the asymmetry degree upon going to dyes with more basic variable terminal group leads to increasing of BLA degree and to decreasing of the charge alternation, mainly, in the open chain. On the other hand, the difference in the electron densities and molecular geometry between DMA-styryls and corresponding OMe-styryls is far lower.

3.4. Relative positions of donor and delocalized levels

Earlier it was established [30] that terminal groups can make the main contributions to the highest occupied MOs of cyanine dyes with a comparatively short polymethine chain (PC). It was shown that the positive charge in the cationic polymethine dye is

localized practically in the open PC. Then, cyanines with two donor terminal groups can be presented as the following system:



where the chain could be treated as an acceptor A. Scheme 3 makes clear this generalization on example of concrete dye – Bim-Me.

It is to be noted that the donor levels, generated predominantly by the lone electron pairs (LEPs) of nitrogen atoms, are positioned higher than the highest delocalized orbital of the main chromophore in cationic cyanine dyes with short PC. Then, we have proposed to consider two highest occupied MOs as donor orbitals (which, of course, are conjugated with delocalized π -electron system of the PC [30]. The donor MOs, $\phi(\text{D}_1)$ and $\phi(\text{D}_2)$, interact between each other to give two new splitting MOs: symmetrical (4) and unsymmetrical (5) linear combinations:

$$\varphi_1 = (2)^{-1/2} \{ \phi(\text{D}_1) + \phi(\text{D}_2) \} \quad (4)$$

$$\varphi_2 = (2)^{-1/2} \{ \phi(\text{D}_1) - \phi(\text{D}_2) \} \quad (5)$$

Fig. 5 shows schematically the splitting of the donor levels in symmetrical (Sym) dyes ($\text{D}_1 = \text{D}_2 = \text{D}$).

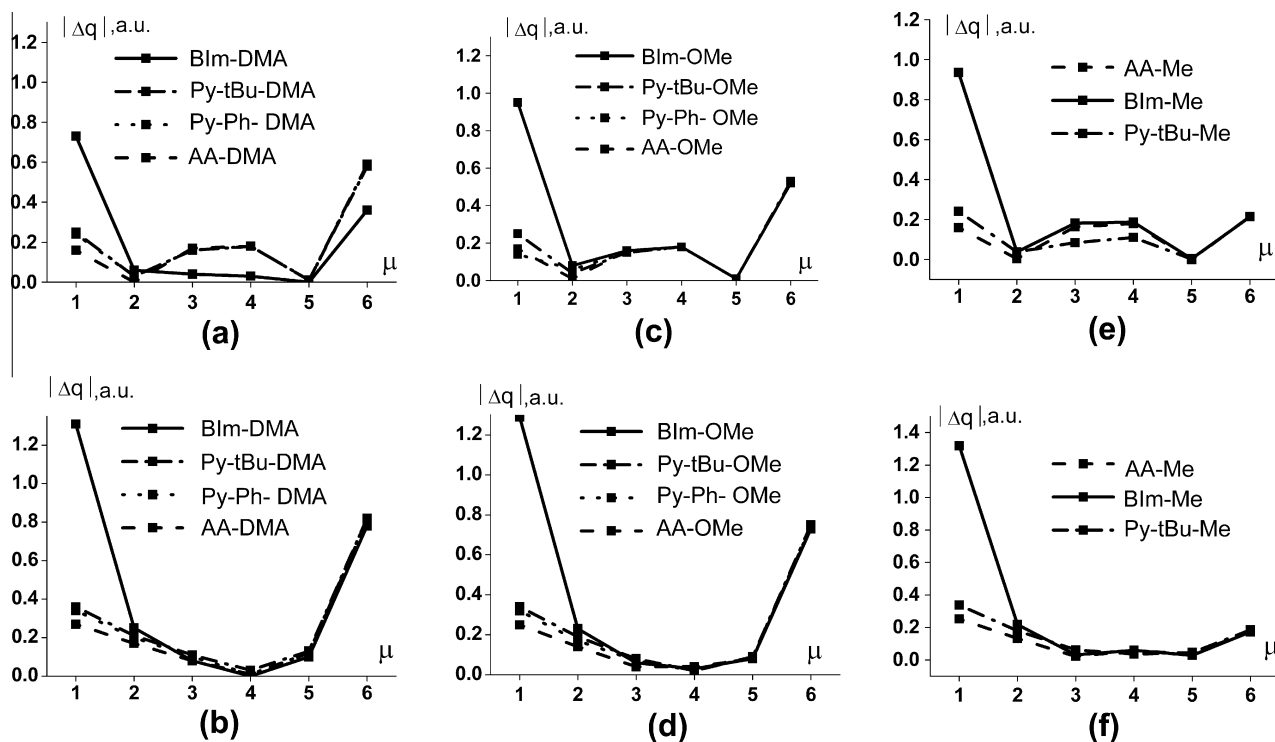


Fig. 3. Alternation of atomic charges Δq_μ for investigated dyes; (a–e) – calculated by DFT method; (b–f) – calculated by HF method. μ is the number of the atoms pair (carbon atom numeration see Scheme 1).

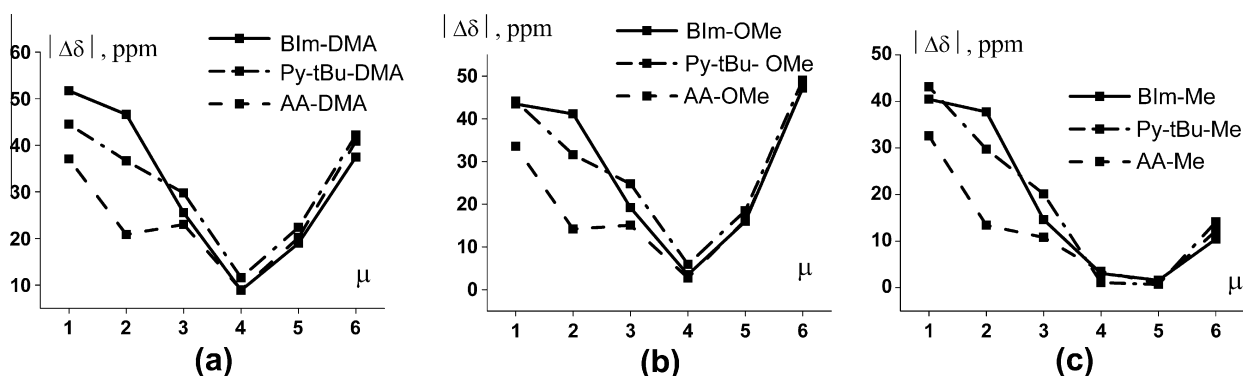
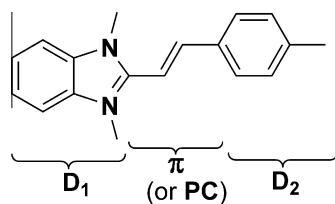


Fig. 4. Alternation of experimental ^{13}C NMR shifts $\Delta\delta_\mu$ (DMSO- d_6) for styryl dyes AA-, Py-tBu- and Blm-: (a) DMA-styryls; (b) OMe-styryls; (c) Me-styryls (carbon atom numeration see Scheme 1).



Scheme 3.

There are three main types of relative positions of splitting donor levels and the higher occupied level of the PC:

- (1) The original donor levels are positioned higher than the level of the PC. The higher occupied level of the dye is the splitting donor levels, φ_1 . We propose to name the symmetrical dyes with such a disposition of the splitting donor levels as *Brooker's dyes* (see Fig. 5a).

- (2) The original donor levels are positioned under the highest occupied level of the PC, nevertheless one of the splitting donor levels proves to be the highest level of the dye, similarly to *Brooker's dyes*. This dye type can be named as *pseudo-Brooker dyes* (see Fig. 5b).
- (3) The original donor levels are positioned too low, so the donor splitting level cannot exceed the highest occupied level of the PC; consequently, the HOMO of this dye type is the delocalized MO of the PC, similarly to the unsubstituted polymethine cation. We propose to name such dyes as *non-Brooker's dyes* (see Fig. 5c).

It has to be noted additionally that the terminal groups in *pseudo-Brooker's* and *non-Brooker's dyes* can contain local MOs positioned higher than the donor orbital of the terminal residues. The first type (Fig. 5a) can be presented by a typical Sym cyanine where $\mathbf{D} = \text{Blm}$. Sym azaazulenecyanine ($\mathbf{D} = \text{AA}$) can be considered

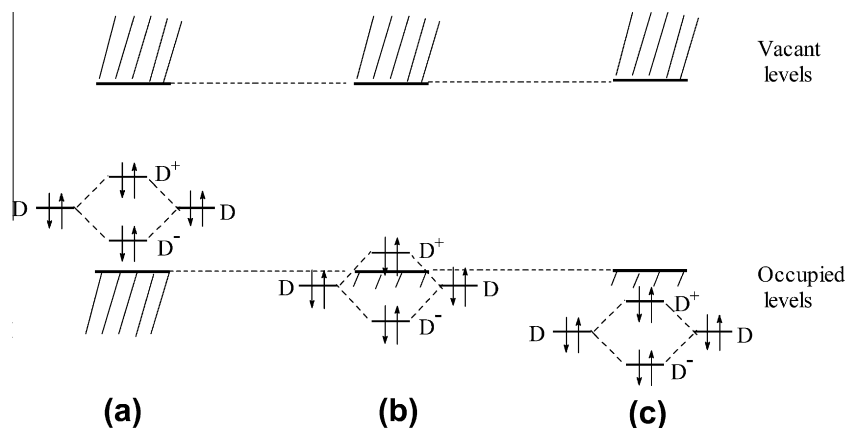


Fig. 5. Splitting of donor levels in symmetrical cationic polymethine dyes: (a) Brooker's type; (b) pseudo-Brooker type; (c) non-Brooker-type.

as an example of the second type of cationic polymethine dyes (Fig. 5b). The detailed investigation presented in our previous papers has shown that the HOMO of the terminal AA residue is a local orbital and therefore does not take part in the conjugation with the PC. Instead of it, HOMO-1 with non-zero coefficient at the carbon atom bonded with the chain is a donor orbital. The interaction of such MOs of both terminal groups in Sym dye ($D = AA$) results in the HOMO, which is one of the splitted donor MOs φ_1 .

Finally, the third type of the relative disposition of donor and delocalized MOs is realized in Sym dye ($D = OCH_3$) with the lone electron pair (LEP) of oxygen atoms providing the donor MOs: both splitting donor levels remain lower than the highest occupied level of the chain.

In unsymmetrical cyanines ($D_1 \neq D_2$), the energies of both donor levels are different. Taking into consideration that the interaction of levels is in inverse proportion to the distance between them, the splitting energy should decrease in unsymmetrical polymethine dyes. Schematically, the dependence of splitting effect on the different distances in two types of unsymmetrical polymethine dyes, DMA-styryl and OMe-styryl, is illustrated in Fig. 6. In the DMA-styryl model, both terminal residues contain nitrogen atoms with their high donor levels hence the distance between both original donor levels is not too large, as one can see from Fig. 6a. Then we would expect that an interaction between them is comparatively high, similarly to symmetrical cyanines. The situation reverses principally in the OMe-styryls model; the corresponding quasi-donor level (generated by the LEP of the oxygen atom) should be disposed rather lower. Fig. 6b demonstrates that the energy of the splitting in such unsymmetrical dye should be practically negligible, in comparison with symmetrical cyanines or even with unsymmetrical dyes, containing both nitrogenous terminal residues (Fig. 6a). Thus, the nature of the HOMO-1 (and hence all electron transition involving this orbital) should be essentially different in DMA-styryls and related OMe-styryls.

Certainly, mentioned above scheme is strongly simplified. The initial donor MOs also interacts with the delocalized MOs of the main chromophore.

The HOMOs in DMA-styryls, with both nitrogen containing residues, are shifted upwards in comparison with the corresponding orbital in OMe-styryls, containing only one heterocyclic nitrogenous terminal group (Fig. 7). At the same time, the position of the lowest vacant level is seen to be less sensitive to the replacement of the dimethylamino group by a methoxy group. Consequently, we can conclude that the methoxyphenylene residue does not produce the high positioned highest occupied level, in contrast to the corresponding nitrogen-containing a DMA terminal group in DMA-styryls. Additionally, it should be noted that the

HOMO-1 in the Py-tBu-OMe with the low basic pyrylium residue is the local MO, as one can see from Fig. 7d, whereas the HOMO-1 in the dye Py-tBu-DMA (Fig. 7c) could be treated (in the framework of our approach) as the second splitting donor orbital, similarly to BIm-DMA.

The scheme of MOs (and hence electron transitions) arrangement in unsymmetrical dyes, especially, in OMe-styryls, becomes considerably more complicated when the variable terminal group R has the local level. So, introducing of phenyl substituents instead of *tert*-butyl-groups in pyrylium heterocycle (upon going from dyes Py-tBu-DMA and Py-tBu-OMe to the corresponding Py-Ph-DMA and Py-Ph-OMe) is accompanied by an appearance of a specific MO located only at the atoms of the terminal group, as one can see comparing Fig. 7c and d with Fig. 7e and f.

This local orbital is the HOMO-1 in both DMA-styryl and OMe-styryl. The next HOMO-2 in DMA-styryl is totally delocalized along the whole chromophore, similarly to the LUMO. The vacant local orbitals obtained from calculation are situated higher and do not take part in the lowest electron transitions.

Similarly, the calculations give the local HOMO-1 in the dyes bearing azaazulenium residue AA-DMA and AA-OMe, as it is demonstrated in Fig. 7g and h.

3.5. A general scheme of electron transitions in styryls of different types: the principal distinctions

The absorption bands observed in visible and near IR spectra of the typical Brooker's symmetrical and unsymmetrical cyanine dyes are known to correspond to the electron transitions involved some highest occupied MOs and some vacant orbitals [5,14–16]. The lowest electron transition is connected practically only with the highest occupied MO and the lowest unoccupied orbital, so that $|S_1\rangle \approx |HOMO \rightarrow LUMO\rangle$. Regarding to the next state, $|S_2\rangle$, its nature depends most commonly on the topology of the terminal groups.

It was shown above (see Fig. 5) that donor terminal groups with their donor MOs generate two highest occupied orbitals. As a rule, in the cationic polymethine dyes, the distance between two lowest vacant levels exceeds considerably the distance between splitted donor levels or even the distance between the highest occupied level and the fifth level below [30]. Then, the first two the lowest transitions involved both $|HOMO\rangle$ and $|HOMO-1\rangle$ in Brooker's type dyes (Fig. 5a) could be treated as coupling transitions. It is obvious that the magnitude of donor levels splitting should be maximal in the symmetrical dyes, because of the degeneration of donor levels. Increasing of the distance between the donor levels in unsymmetrical dyes should be accompanied by decreasing of

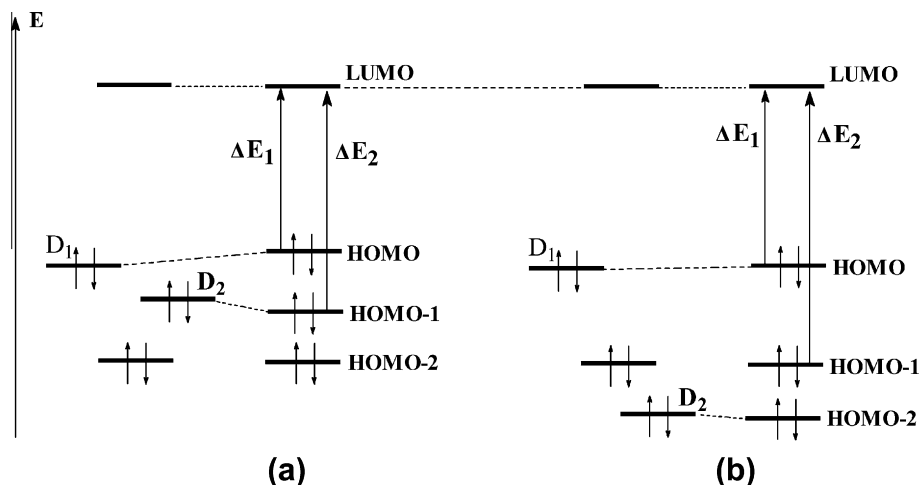


Fig. 6. Schematic disposition of delocalized and donor (D_1 and D_2) levels as well as two first electron transitions in DMA-styryl (a) and OMe-styryl (b).

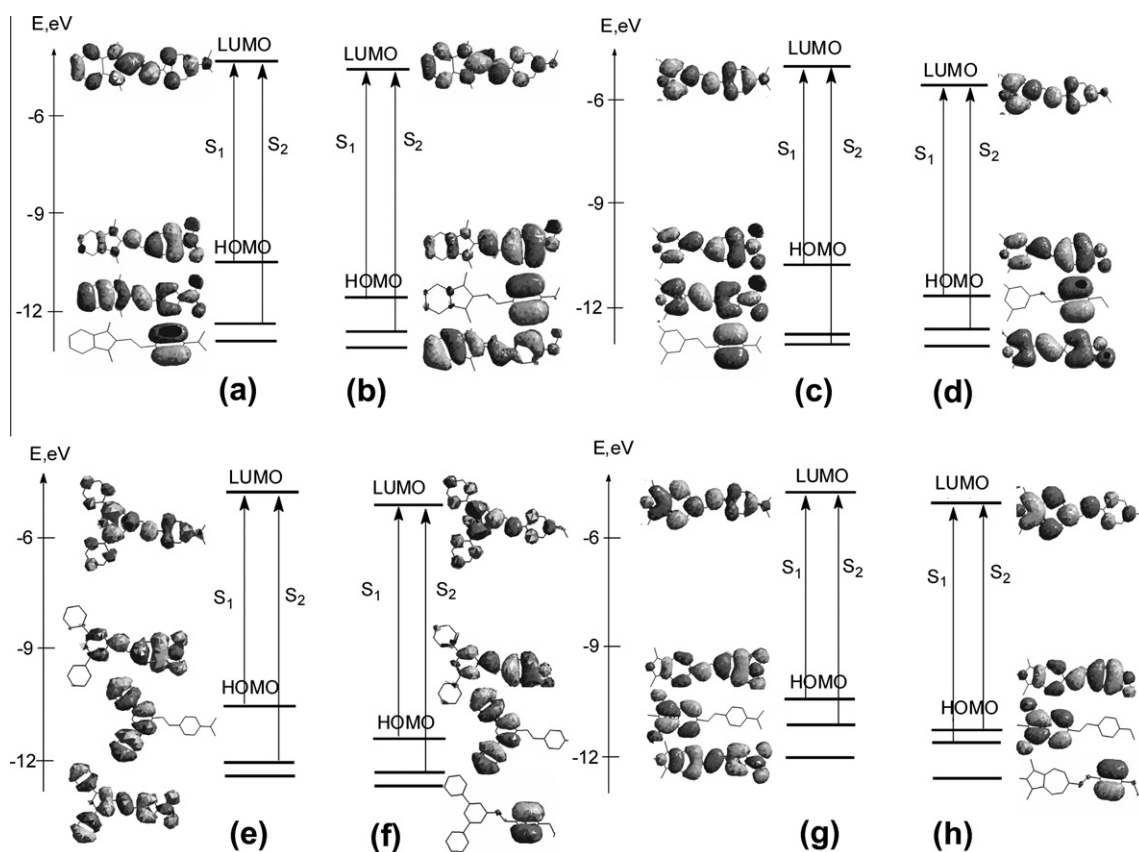


Fig. 7. Shapes of the frontier and nearest MOs and the two lowest electron transitions in dyes Blm-DMA (a), Blm-OMe (b), Py-tBu-DMA (c), Py-tBu-OMe (d), Py-Ph-DMA (e), Py-Ph-OMe (f), AA-DMA (g), and AA-OMe (h). AM1 method.

the splitting energy. Then, one could expect two main features that distinguish DMA-styryls from OMe-styryls:

- (1) The two lowest electron transitions $S_0 \rightarrow S_1$ and $S_0 \rightarrow S_2$ in DMA-styryls as dyes with highly positioned donor levels of both terminal groups, are coupled transitions involved splitted donor levels and the same lowest vacant level (Fig. 5a), similarly to the symmetrical cyanine. Whereas $S_0 \rightarrow S_2$ transition in OMe-styryls (Fig. 5b) should be connected with the delocalized MO of the chain.

- (2) The strong interaction between two donor levels and those owing to their splitting in the DMA-styryls results in the appreciable decreasing of the first electron transition energy and hence in the comparatively long wave (deep) color of these dyes. The situation is different for methoxy substituted analogous, where the first electron transition depends practically on the one donor quasi-local level position without essential additional decreasing of the transition energy by the interaction with another donor level generated by the LEP of the oxygen atom (Fig. 6a and b).

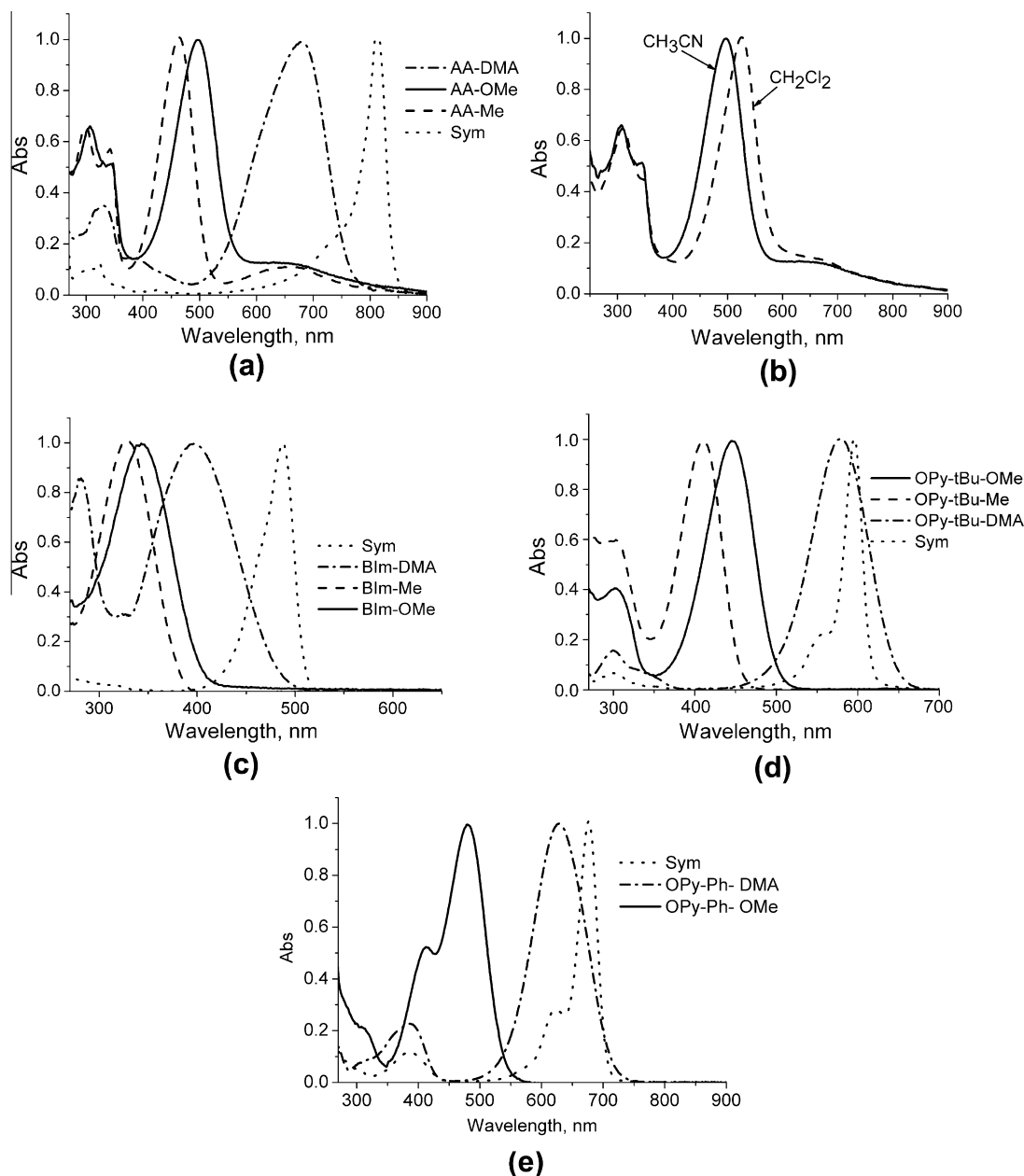


Fig. 8. Normalized absorption spectra of investigated dyes and symmetrical dyes Sym ($D_1=D_2=D$) recorded in acetonitrile: (a) AA-derivatives; (c) Blm derivatives; (d) Py-tBu derivatives; (e) Py-Ph derivatives. (b) Shows AA-OMe dye in different solvent, acetonitrile (CH_3CN) and methylene chloride (CH_2Cl_2).

Of course, this scheme is considerably simplified, however, such theoretical assumption helps to interpret the spectral data correctly. On the other hand, the above mentioned scheme (Fig. 5) becomes complicated, when the terminal groups have a high positioned local MO. As a result, the nature of the lowest transitions and hence the shape of the spectral bands could undergo the considerable transformations.

3.6. Absorption spectra and a nature of electron transitions

One can see from Fig. 8 that the typical high intensive and high selective long wavelength absorption bands are observed in the spectra of all symmetrical dyes Sym ($D_1=D_2=D$). The band maximum is regularly red shifted in series Sym: $D = \text{AA}$ (Fig. 8a), $D = \text{Blm}$ (Fig. 8c), $D = \text{Py-tBu}$ (Fig. 8d), $D = \text{Py-Ph}$ (Fig. 8e), in respect to increasing of the effective length of the terminal residue. Introducing two phenyl substituents in the pyrylium heterocycle

(Fig. 8e) causes not only the bathochromic shift (82 nm) of the first spectral band, but also the appearance of the comparatively low intensive absorption band with the maximum at 386 nm, which corresponds to the practically degenerated electron transitions, $S_0 \rightarrow S_2$ and $S_0 \rightarrow S_3$ (Table 3), involving the local MOs HOMO-1 (their shapes are the same in DMA-styryls and OMe-styryl Py-Ph-DMA, Py-Ph-OMe, see Fig. 7e and f). Similarly, it was established earlier, [15] that the short wavelength absorption in the spectra of dye Sym, $D = \text{AA}$ is connected with the local transitions.

Aiming to compare DMA-styryls and OMe-styryls we discuss their spectra and two lowest electron transitions, taking into consideration the nature of the variable terminal groups.

3.6.1. Dyes derivatives of cyclohepta[c]pyrrolium (2-azaazulenium dyes)

The particular emphasis of our investigation of the influence of the local level on the absorption spectra was devoted to the pair of

Table 3Wavelengths (λ) and oscillator strengths (f) of the lowest electron transitions of studied dyes calculated by TD DFT and AM1 methods.

Dye	Transition	TD DFT			AM1		
		λ (nm)	f	Main configuration	λ (nm)	f	Main configuration
Blm-DMA	S0 \rightarrow S1	467	1.160	0.79 H \rightarrow L>	434	1.328	0.91 H \rightarrow L>
	S0 \rightarrow S2	355	0.060	0.81 H-1 \rightarrow L>	268	0.028	0.88 H-1 \rightarrow L>
Blm-OMe	S0 \rightarrow S1	431	0.990	0.81 H \rightarrow L>	355	0.870	0.95 H \rightarrow L>
	S0 \rightarrow S2	359	0.016	0.95 H-1 \rightarrow L>	268	0.102	0.91 H-1 \rightarrow L>
Py-t-Bu-DMA	S0 \rightarrow S1	489	1.160	0.92 H \rightarrow L>	494	1.578	0.92 H \rightarrow L>
	S0 \rightarrow S2	432	0.003	0.95 H-1 \rightarrow L>	317	0.074	0.70 H-2 \rightarrow L>
Py-t-Bu-OMe	S0 \rightarrow S1	464	0.990	0.76 H \rightarrow L>	455	1.315	0.92 H \rightarrow L>
	S0 \rightarrow S2	416	0.021	0.94 H-1 \rightarrow L>	309	0.074	0.65 H-1 \rightarrow L>
Py-Ph-DMA	S0 \rightarrow S1	556	1.200	0.76 H \rightarrow L>	548	1.557	0.87 H \rightarrow L>
	S0 \rightarrow S2	485	0.010	0.89 H \rightarrow L + 1>	381	0.586	0.88 H-1 \rightarrow L>
	S0 \rightarrow S3	458	0.210	0.82 H-1 \rightarrow L>	300	0.015	0.78 H \rightarrow L + 1>
Py-Ph-OMe	S0 \rightarrow S1	525	1.050	0.80 H \rightarrow L>	478	1.309	0.86 H \rightarrow L>
	S0 \rightarrow S2	476	0.210	0.89 H-1 \rightarrow L>	398	0.520	0.89 H-1 \rightarrow L>
	S0 \rightarrow S3	459	0.005	0.82 H-3 \rightarrow L>	336	0.002	0.68 H-2 \rightarrow L>
AA-DMA	S0 \rightarrow S1	627	0.011	0.93 H-1 \rightarrow L>	555	1.487	0.85 H \rightarrow L>
	S0 \rightarrow S2	552	1.310	0.74 H \rightarrow L>	534	0.083	0.91 H-1 \rightarrow L>
	S0 \rightarrow S3	519	0.001	0.96 H-2 \rightarrow L>	366	0.176	0.79 H \rightarrow L + 1>
AA-OMe	S0 \rightarrow S1	636	0.012	0.93 H-1 \rightarrow L>	557	0.059	0.93 H-1 \rightarrow L>
	S0 \rightarrow S2	524	1.150	0.74 H \rightarrow L>	496	1.282	0.88 H \rightarrow L>
	S0 \rightarrow S3	432	0.013	0.89 H-2 \rightarrow L>	369	0.292	0.82 H-2 \rightarrow L>

the related dyes AA-DMA and AA-OMe (Fig. 8a). Taking into consideration that electron transition, which involves occupied local orbital corresponds to the lowest transition in the origin salt of the variable heterocycle, and remembering that the azaazulenium salt absorbs rather deeply (634 nm [15]), we have expected the most unusual phenomena in the spectrum of DMA-styryl and, especially, methoxystyryl dye, which are derivatives of the non-alternant heterocycle \rightarrow azaazulene. Although the local level is seen from Fig. 7g and h to be not the highest occupied level, nevertheless the energy of the local transition can be lower than the energy of the transition between the delocalized frontier levels, as it is obtained by the calculations (Table 3). This is connected with the different contribution of the integrals of the electron interaction, K_{ij} and J_{ij} , in the formulas for the electron transition between any i - and j -MOs (6) for the delocalized and local transitions.

$$\Delta E_{i \rightarrow j} = \varepsilon_j - \varepsilon_i + 2K_{ij} - J_{ij} \quad (6)$$

here ε_j and ε_i are energies of the orbital involving in the transition.

One could see from Table 3 that both methods predict a significant decreasing of the oscillator strengths (f) for the transition from the local HOMO-1 in respect to the transition that involves HOMO. In styryl AA-DMA, the distance between the first and the second transitions is minimal. The AM1 predicts that the local transitions should be the second transition shifted hypsochromically at 21 nm, in respect to the first transition, whereas the TD DFT method gives the opposite disposition of the transitions |HOMO> \rightarrow |LUMO> and |HOMO-1> \rightarrow |LUMO> with the larger distance between them: 75 nm. Both methods predict negligible oscillator strength for the local transition. Thus, we cannot establish the position of the virtual spectral band corresponding to the local transition. We could only suppose that some broadening of the long wavelength band with the maximum at 681 nm is likely to be connected with nearby two electron transitions.

For methoxystyryl AA-OMe, both methods have predicted unambiguously the lower energy of the local transition with low oscillator strength so, that corresponding low intensive spectral band should be shifted bathochromically: at 112 nm (TD DFT) or 61 nm (AM1). I.e. the inversion of two lowest electron transitions of different nature should be observed:

- (1) the delocalized transition manifesting itself as an intensive cyanine-like spectral band;
- (2) the local transition, which exhibit the comparatively low and wide band.

To confirm our theoretical assumption, we have synthesized not only AA-OMe, but also the corresponding dye AA-Me without any donor group with the LEP. The measured absorption spectra of both dyes are seen from Fig. 8a to support our hypothesis. One can clearly see that going from AA-DMA to AA-OMe is accompanied by the drastic transformation of the absorption spectrum: the short wavelength band becomes the typical cyanine-like band with its maximum at 497 nm, whereas the long wavelength band is wide and low intense, its shape being similar to the first band in the spectrum of azaazulenium salt. Also, in order to show that the shape of the absorption spectrum of the AA-OMe dye is the consequence of the peculiarities of electronic structure but not the influence of the solvent [31], we used two different solvent acetonitrile (CH_3CN) and methylene chloride (CH_2Cl_2). As it seen from Fig. 8b, absorption spectra forms are similar and show the same tendency, the first electron transition is not intensive, only some shift of the maximum of the next intensive band is present.

Thus, basing on the general assumption about the relative dispositions of the electron transition of different nature in dyes with the high positioned local level as well as on the calculated data, obtained in both quantum-chemical methods, we conclude that the long wavelength spectral band with its maximum approximately at 680 nm corresponds to electron transition involving the local orbital (HOMO-1), while the second narrow and high intense band with its maximum at 497 nm is generated by the transition between the totally delocalized frontier MOs. As an additional confirmation of this conclusion about the nature of two spectral bands, the spectrum of dye AA-Me could be considered: the spectra of both dye AA-OMe and its analogue AA-Me are practically the same, only the short wavelength cyanine-like band is shifted slightly hypsochromically and the local transition manifests itself more clearly – as a separated wide long wavelength band with its maximum at 660 nm. Consequently, the performed investigations confirm undoubtedly our statement about the inversion of cyanine-like and local electron transitions which observed as a principal change of the shape of spectral bands in the absorption spectra.

Besides, the compounds AA-OMe and AA-Me are the first dyes derivatives of AA, in which the local transition manifest itself as an individual spectral band.

3.6.2. Dyes derivatives of benzimidazolium

As it was shown above, the styryl Blm-DMA is a typical Brooker's cyanine containing both nitrogenous terminal groups: a high basic Blm residue and a low basic p-dimethylaminophenylene residue. Both HOMO and HOMO-1 involved in $S_0 \rightarrow S_1$ and $S_0 \rightarrow S_2$ transitions are totally delocalized MOs, the splitting between them is comparatively not large. Then, the two lowest electron transitions are described correctly by the scheme presenting in Fig. 5a, similarly to other Brooker's unsymmetrical polymethine dyes. We can estimate quantitatively the degree of asymmetry of dye Blm-DMA using the deviation D calculated by Brooker's formulae:

$$D = (\lambda_1 + \lambda_2)/2 - \lambda_{as} \quad (7)$$

where λ_{as} is the absorption maximum of the unsymmetrical dye while λ_1 and λ_2 are the maxima of the corresponding symmetrical parent molecules.

The measured spectra of the corresponding dyes give: $D = 150$ nm. Such large value points to a considerable difference in basicities of both terminal groups in Blm-DMA styryl.

The calculation results obtained by the means of time depended (TD) DFT method are seen from Table 3 and give the second transition $S_0 \rightarrow S_2$ that involves the |HOMO-1>. Then, this transition could be treated as the second splitting transition. It follows from Table 3 that it should be shifted hypsochromically upon 112 nm, but the calculated oscillator strength f_2 is too small this transition to be observed in the absorption spectra. It should be noticed that the semi-empirical AM1 method gives the second transition to involve the |HOMO-1> too, nevertheless the distance between the first and second transition is also rather large: 166 nm.

One can see from Fig. 8c that going from Blm-DMA dye to its methoxy analogue Blm-OMe is accompanied by a considerable hypsochromic effect. As far as the interaction of the donor levels in methoxystyryls should be significantly smaller, in comparison with corresponding DMA-styryls (compare Fig. 6a and b), the energy of the first electron transition should be considerably higher, and hence the absorption band maximum is necessarily shifted in the short wavelength spectral region. The observed hypsochromic effect is 54 nm (3953 cm^{-1}) (see Fig. 8c).

It has been observed that the calculated spectral effect is lower for TD DFT – 36 nm and higher for AM1 method – 79 nm, that is connected, first of all, with a considerable discordance between the calculated wavelength of the first electron transition λ_{calc} and the observed spectral band maximum λ_{max} for the styryl with both nitrogenous terminal groups, while the corresponding values, λ_{calc} and λ_{max} for OMe-styryl are seen from Table 3 and Fig. 8c to be comparatively close.

The calculation gives the second transition $S_0 \rightarrow S_2$ in OMe-styryl Blm-OMe that involves the local orbital |HOMO-1>, as one can see from Fig. 7b. The corresponding spectral band should appear at 359 nm (TD DFT) but none appreciable absorption is observed in the spectrum up to 300 nm, that could be connected with too low oscillator strength ($f_2 = 0.016$).

Such considerable hypsochromic shift of the long wavelength absorption band in spectrum of Blm-OMe, in comparison with the spectrum of its nitrogen-containing analogue Blm-DMA, confirms the hypothesis about the change of the nature of the two lowest electron transitions in related dyes Blm-OMe and Blm-DMA. We could even assume that the first electron transition in the OMe-styryl is similar to that in the corresponding Blm salt, but with exo-cyclic conjugated substituent. To confirm this idea, the corresponding dye Blm-Me without any second donor residue was synthesized. One could see from Fig. 8c that spectral band for

dye Blm-Me is shifted hypsochromically in comparison with dye Blm-OMe only by 14 nm and reproduces its band shape. Then we can argue that the methoxy group in dye Blm-OMe practically does not affect the electron transition, in contrast to dye Blm-DMA, in which the presence of two nitrogenous terminal groups with their high positioned donor levels provides a considerable splitting of the donor energy levels and hence appreciable raising of the high-est occupied level of the dye.

3.6.3. Dyes derivatives of 2,6-di-tert-Bu-pyrylium

Similarly to the large bathochromic shift of the long wavelength band maximum observed in the absorption spectra of symmetrical dyes Sym upon replacing of benzimidazolium terminal groups by the 2,6-di-*t*Bu-pyrylium residues, a considerable spectral effect is seen from Fig. 8c and d to be observed upon going to: Blm-DMA \rightarrow Py-*t*Bu-DMA and Blm-OMe \rightarrow Py-*t*Bu-OMe. Nevertheless, the analysis of the measured spectral data and corresponding calculated results shows that the nature of the first electron transitions in unsymmetrical dyes Py-*t*Bu-DMA and Py-*t*Bu-OMe is the same as in corresponding dyes Blm-DMA and Blm-OMe. I.e., 2,6-di-*t*Bu-pyrylium terminal group does not produce any specific additional MOs which could principally change the type of the first and the second electron transitions. The measured spectrum of styryl Py-*t*Bu-DMA and the spectrum of the corresponding parent symmetric cyanine dyes exhibit also the reasonable deviation: $D = 21.5$ nm, however, the value D is less than this parameter for the styryl Blm-DMA with high basic variable terminal groups. Consequently, decreasing of the deviation points to decreasing of the basicity of 2,6-di-*t*Bu-pyrylium terminal group, that agrees with the conclusion about the comparatively low basic properties of the pyrylium heterocycle, obtained by the analysis of the charge distribution.

Spectral effect upon going from styryl Py-*t*Bu-DMA to dye Py-*t*Bu-OMe, 131 nm (5090 cm^{-1}), is also large, but it is smaller than in the pair of dyes Blm-DMA \rightarrow Blm-OMe. At least, the replacement of $-\text{OCH}_3$ group by the methyl substituent in dye Py-*t*Bu-Me causes only the relative insignificant hypsochromic shift of the long wavelength band maximum without appreciable change of its shape, in comparison with dye Py-*t*Bu-OMe, supporting the statement about the same nature of the first electron transition in these dyes.

3.6.4. Dyes derivatives of 2,6-di-Ph-pyrylium

The regularities concerning the long wavelength absorption band observed for the pair of dyes DMA-styryl and OMe-styryl discussed above remain the same also for Py-Ph-DMA and related Py-Ph-OMe dye, only the absorption maximum is blue shifted (from 628 nm to 481 nm). The calculated wavelength of the first electron transition (see Table 3) differs somewhat from the experimental result. Nevertheless, both methods help to interpret the nature of transitions correctly, as well as to give the considerable distance between the first and the next transition.

The relatively large deviation that appears in the spectrum of styryl: $D = 12.5$ nm, testifies about the difference in the basicities of terminal groups. Naturally, going from DMA-styryl to OMe-styryl is accompanied by a considerable hypsochromic shift of the band maximum that points at the difference of the nature of the first electron transitions, similarly to the dyes mentioned above (Py-*t*Bu- and Blm-).

However, it was shown above (see Fig. 7c) that introducing of two phenyl substituents instead of *tert*-Bu groups in the pyrylium heterocycle leads not only to exceeding of the total length of the conjugated system, but to the appearance of the high positioned level, which corresponds to the HOMO-1, located entirely on 2,6-di-Ph-pyrylium residue in both styryl Py-Ph-DMA and related dye Py-Ph-OMe. Then, the electron transition involving the local

MO should appear in the spectra. One can see from Fig. 8e that separated appreciable spectral band with maximum at 386 nm is observed in the short wavelength region, similar to the spectrum of symmetrical pyrylotrimethine cyanine Sym ($D = \text{Py-Ph}$). The calculation by AM1 method of dye Py-Ph-DMA is seen from Table 3 and gives the wavelength of the second transition: 381 nm that is close to the experimental maximum. This transition is described by only one configuration: local HOMO-1 \rightarrow LUMO. Also, AM1 method predicts a comparatively high oscillator strength that agrees with sufficient intensity of this transition to manifest itself as a separated band in the spectrum. The distance between two first maxima, corresponding to the transitions from the highest splitting donor orbital (HOMO) and from local orbital (HOMO-1), is 242 nm, whereas the calculations give the smaller value: 167 nm, that is connected with the divergence between the experimental and calculated wavelengths of the first transition: $\approx 628 \text{ nm} - 548 \text{ nm} = 80 \text{ nm}$.

At the same time, the wavelength of the local transition obtained by TD DFT calculation far exceeds the experimental value observed as a maximum of the second spectral band. Besides, this method gives that the local transition, $|\text{HOMO}-1\rangle \rightarrow |\text{LUMO}\rangle$ is the third transition with a comparatively low oscillator strength, while the second transition with negligible value f_2 involves the HOMO and the next vacant orbital ($\text{LUMO} + 1$), in contrast to AM1 method (compare the corresponding data in Table 3). As far as both quantum-chemical methods give too small oscillator strength for the transition connected with delocalized orbitals $|\text{HOMO}\rangle \rightarrow |\text{LUMO} + 1\rangle$ and hence this transition does not manifest itself in the absorption spectrum, we cannot state what method is more correct in the calculation of the highest electron transitions.

Both methods necessarily predict a substantial increasing of the energy of the first electron transition upon going from the styryl Py-Ph-DMA to its analogue Py-Ph-OMe, that should be observed in the absorption spectra as a hypsochromic shift of the long wavelength band maximum, on 70 nm (AM1) and 31 nm (TD DFT). Comparing the corresponding values from Tables 1 and 3, one can see that experimental effect exceeds the calculated magnitude. In regards to the local transition, $|\text{HOMO}-1\rangle \rightarrow |\text{LUMO}\rangle$, both methods predict close bathochromic shift of the corresponding spectral band maximum: 17 nm (AM1) and 18 nm (TD DFT).

4. Conclusion

Thus, both quantum-chemical and spectral investigation of dimethylaminostyryl and methoxystyryl dyes bearing 2-azaazulenium moiety as well as their analogues with benzimidazolium and pyrylium residues have shown that these two types of extremely unsymmetrical cyanines differ between each other only slightly in the ground state with respect to the charge distribution and molecular geometry. In contrast, their spectral properties demonstrate a considerable difference between styryls and methoxystyryls because of the lowest disposition of level of LEP of oxygen atom and hence, limiting basicity of the p-methoxyphenylene residue. Then, the classification of the terminal groups of cyanine dyes and hence the classification of types of unsymmetrical cyanines should be extended by taking into consideration such oxygen-containing terminal groups. It is shown that the appearance of the high-positioned local level generated by AA terminal group caused the inversion of the delocalized and quasi-local electron transitions

in AA-methoxystyryl and hence drastic changes in its absorption spectrum.

Acknowledgement

Financial support by Science and Technology Centre in Ukraine (STCU Project 4270) is gratefully acknowledged.

Appendix A. Supplementary material

Supplementary data associated with this article can be found, in the online version, at <http://dx.doi.org/10.1016/j.molstruc.2012.08.034>.

References

- [1] T. Deligeorgiev, A. Vasilev, S. Kaloyanova, *Color. Technol.* 126 (2010) 55–80.
- [2] L.G.S. Brooker, *Rev. Mod. Phys.* 14 (1942) 275–293.
- [3] S. Daehne, *Science* 199 (1978) 1163–1167.
- [4] G. Bach, S. Daehne, in: M. Sainsbury (Ed.), *Rodd's Chemistry of Carbon Compounds*, vol. IVB, Elsevier, Amsterdam, 1997 (Chapter 15).
- [5] N. Tyutyulkov, J. Fabian, A. Mehlhorn, F. Dietz, A. Tadjer, *Polymethine Dyes: Structure and Properties*, St. Kliment Ohridski University Press, Sofia, 1991. p. 328.
- [6] A. Mishra, *Chem. Rev.* 100 (2000) 1973–2011.
- [7] Lan-Ying Wang, Qin-Wen Chen, Gao-Hong Zhai, *Dyes Pigments* 72 (2007) 357–362.
- [8] Shakir T. Abdel-Halim, Mohamed K. Awad, *J. Mol. Struct.* 920 (2009) 332–341.
- [9] M. Dakovic, H. Cicak, Z. Soldin, *J. Mol. Struct.* 938 (2009) 125–132.
- [10] F.M. Hamer, in: A. Weissberger (Ed.), *The Cyanine Dyes and Related Compounds in the Chemistry of Heterocyclic Compounds*, vol. 18, Wiley-Interscience, New York, 1964.
- [11] H. Kuhn, *J. Chem. Phys.* 17 (1949) 1198–1221.
- [12] N.S. Bayliss, *J. Chem. Phys.* 16 (1948) 287–292.
- [13] W.T. Simpson, *J. Am. Chem. Soc.* 73 (1951) 5359–5363.
- [14] A.D. Kachkovsky, *Russ. Chem. Rev.* 66 (1997) 647–664.
- [15] J. Bricks, A. Ryabitskii, A. Kachkovskii, *Eur. J. Org. Chem.* (2009) 3439–3449.
- [16] J. Bricks, A. Ryabitskii, A. Kachkovskii, *Chem. Eur. J.* 16 (2010) 8785–8796.
- [17] A.V. Stanova, A.V. Ryabitskii, V.M. Yashchuk, O.D. Kachkovskii, A.O. Gerasov, *J. Mol. Struct.* 988 (2011) 102–110.
- [18] A.L. Davis, J. Keeler, E.D. Laue, D. Moskau, *J. Magn. Reson.* 98 (1992) 207–216.
- [19] D.J. States, R.A. Haberkorn, D.J. Ruben, *J. Magn. Reson.* 48 (1982) 286–292.
- [20] A. Bax, G.A. Morris, *J. Magn. Reson.* 42 (1981) 501–505.
- [21] M.J. Frisch, G.W. Trucks, H.B. Schlegel, G.E. Scuseria, M.A. Robb, J.R. Cheeseman, J.A. Montgomery Jr., T. Vreven, K.N. Kudin, J.C. Burant, M. Millam, S.S. Iyengar, J. Tomasi, V. Barone, B. Mennucci, M. Cossi, G. Scalmani, N. Rega, G.A. Petersson, H. Nakatsuji, M. Hada, M. Ehara, K. Toyota, R. Fukuda, J. Hasegawa, M. Ishida, T. Nakajima, Y. Honda, O. Kitao, H. Nakai, M. Klene, X. Li, J.E. Knox, H.P. Hratchian, J.B. Cross, C. Adamo, J. Jaramillo, R. Gomperts, R.E. Stratmann, O. Yazyev, A.J. Austin, R. Cammi, C. Pomelli, J.W. Ochterski, P.Y. Ayala, K. Morokuma, G.A. Voth, P. Salvador, J.J. Dannenberg, V.G. Zakrzewski, S. Dapprich, A.D. Daniels, M.C. Strain, O. Farkas, D.K. Malick, A.D. Rabuck, K. Raghavachari, J.B. Foresman, J.V. Ortiz, Q. Cui, A.G. Baboul, S. Clifford, J. Cioslowski, B.B. Stefanov, G. Liu, A. Liashenko, P. Piskorz, I. Komaromi, R.L. Martin, D.J. Fox, T. Keith, M.A. Al-Laham, C.Y. Peng, A. Nanayakkara, M. Challacombe, P.M.W. Gill, B. Johnson, W. Chen, M.W. Wong, C. Gonzalez, J.A. Pople, *GAUSSIAN 03*, Revision B.05, Gaussian, Inc., Pittsburgh PA, 2003.
- [22] A.D. Becke, *J. Chem. Phys.* 98 (1993) 5648–5652.
- [23] J.E. Carpenter, F. Weinhold, *J. Mol. Struct.* 169 (1988) 41–62.
- [24] F.M. Hamer, in: A. Weissberger (Ed.), *The Cyanine Dyes and Related Compounds in the Chemistry of Heterocyclic Compounds*, vol. 18, Wiley-Interscience, New York, 1964, p. 398.
- [25] A. Ryabitskii, J. Bricks, A. Kachkovskii, *J. Mol. Struct.* 1007 (2012) 52–62.
- [26] R. Wizinger, P. Ulrich, *Helv. Chim. Acta* 39 (1956) 207–216.
- [27] W. Diltz, J. Fischer, *Chem. Ber.* 57 (1924) 1653–1656.
- [28] J.S. Craw, J.R. Reimers, G.B. Backs, *Chem. Phys.* 167 (1992) 77–99.
- [29] J.S. Craw, J.R. Reimers, G.B. Backs, *Chem. Phys.* 167 (1992) 101–109.
- [30] S. Webster, J. Fu, L.A. Padilha, H. Hu, O.V. Przhonska, D.J. Hagan, E.W. Van Stryland, M.V. Bodnar, Yu L. Slominsky, A.D. Kachkovskii, *J. Lumin.* 128 (2008) 1927–1936.
- [31] Julia L. Bricks, Juri L. Slominskii, Margarita A. Kudinova, Alexei I. Tolmachev, Knut Rurack, Ute Resch-Genger, Wolfgang Rettig, *JPPA* 132 (2000) 193–208.